Jurnal Geografi Gea

Journal homepage https://ejournal.upi.edu/index.php/gea

Comparison of Global and Local Deterministic Interpolation Methods to Predict Spatial Distribution of Ni, Fe, and MgO in Nickel Laterite Deposits

Hendro Purnomo[1], Shilvyanora Aprilia Rande[2], R. Andy Erwin Wijaya[3], Faisol Mukarrom[4]

[1234] Department of Mining Engineering, Institut Teknologi Nasional Yogyakarta, Jl Babarsari, Caturtunggal, Depok, Sleman Yogyakarta, Indonesia

Correspondence: E-mail: [1]Hendro.purmomo@itny.ac.id

ABSTRACT

The selection of an interpolation method that complies with the availability of data, to map the grade distribution of mineral commodities, is an important issue in every stage of exploration in the mining industry. A reliable method can produce accurate predictions of the grade distribution of deposits so that it can be used to properly evaluate the economic potential of a mineral deposit. The objective of this research was to compare the performance of four deterministic interpolation methods, including Global Polynomial Interpolation (GPI), Radial Basis Function (RBF), Inverse Distance Weighting (IDW), and Local Polynomial Interpolation (LPI), to map the distribution of Ni, Fe, and MgO. The evaluation of the interpolation results was carried out using the cross-validation technique through the statistical parameters Mean Error (ME), Root Mean Square Error (RMSE), and Mean Relative Error (MRE). The results of the comparison show that the performance of the RBF method is the most accurate as indicated by the lowest RMSE and MRE values, or the ME value that is closest to zero. It can be concluded that the RBF interpolation technique is the best method for predicting the spatial distribution of Ni, Fe, and MgO grades in this study area

ARTICLE INFO

Article History:
Submitted/Received: 28 August 2023
Accepted: 27 September 2023
First Available online: 30 April 2024
Publication Date: 30 April 2024

Keyword:
Interpolation,
Deterministic,
GPI,
RBF,
IDW,
LPI.

1. INTRODUCTION

Along with the rapid development of the manufacture of batteries for electric vehicles and the increasing demand for stainless steel, this has affected the development of the world's nickel mining industry (Konig U, 2021). Approximately 60% to 70% of the global nickel resources come from laterite deposits and the remainder comes from nickel sulfide (Butt. C.R.M and Cuzel. D, 2013, Garvin. M.M, and Simon. M.J. 2014, Guo. Z et al, 2017). However, currently around 40% of world nickel production comes from laterite deposits and 60% comes from nickel sulfide (Konig U, 2021). It is estimated that in 2025 the world's nickel demand for battery manufacture will increase by approximately 15%, and this additional supply of nickel will be mined mainly from lateritic deposits (Konig U, 2021). On the other hand the mining activities will cause change the landscape such as topography, vegetation cover, hydrological patterns, and damage to soil structures (Isdianti, A.R et al, 2022). Currently nickel laterite is more attractive not only because it has a large amount of resources globally, but also because of the continuing increase in the cost of mining nickel sulphide and the environmental pollution caused by its production process (Zhang et al, 2019, Yan N et al, 2015).

Nickel laterite is formed from the weathering of ultramafic rocks in humid tropical climates. The type of rock and climate during the lateritization process will affect the type of mineralogy and grade of ore in nickel laterite deposits (Konig U, 2021). Nickel is hosted on minerals such as oxides, clay silicates, and hydrous Mg silicates (Butt C R M and Cluzel D, 2013) . In general, the profile of nickel laterite deposits from bottom to top is: bedrock consisting of ultramafic or partially weathered ultramafic rocks, saprolite or silicate zone characterized by Mg-silicate minerals such as serpentine and garnierite, and limonite or oxide zones with the dominant composition of iron oxyhydroxides, especially mineral goethite, hematite, and maghemite (Golightly J, 1981, Elias M, 2002). Approximately 85% of the world's nickel laterite resources are located in Cuba, New Caledonia, Indonesia, Philippines, Vietnam and Brazil (Butt C R M and Cluzel D., 2013., Nkrumah P.N et al, 2016). Indonesia is one of the world's largest suppliers of lateritic nickel ore where its resources are found in the eastern part of Indonesia, especially in Sulawesi and the Maluku islands (Farrokhpay S et al, 2019, Zhou S W et al, 2017).

The main issue in assessing mineral resources is how to predict the spatial distribution of the grades of element commodities in mineral deposits (Qu H et al, 2021, Daya, 2012, Li X L et al, 2010). Therefore, the selection of an appropriate interpolation method according to the amount and distribution of available data is important. Reliable prediction of grade distribution and resource estimation is used to evaluate the economic potential of a mineral deposit (Qu H et al, 2021). Accurate prediction results will affect the potential number of reserves and the economic potential of resources in an area (Zhang J.D,et al, 2002). The spatial interpolation method is a technique for estimating locations where there is no data by using existing observation data around the estimated target point (Losser et al, 2014, Chai. H et al, 2011). Spatial interpolation methods that are known at this time include geostatistical methods, consisting of ordinary kriging, simple kriging, universal kriging, Co kriging, indicator kriging and others, and deterministic interpolation methods consisting of global polynomial interpolation (GPI), Local polynomial interpolation (LPI), inverse distance weighted interpolation (IDW), and radial basis function (RBF) (Yong X et al, 2016). Geostatistical methods have been widely accepted for predicting spatial distribution and estimating resources in the mining industry. In its calculations, this method is very dependent on the correlation of spatial data reflected by the variogram model. However, in reality it is not always possible to construct an

DOI: https://doi.org/10.17509/gea.v24i1.61886
p- ISSN 2776-608X e- ISSN 2776-5970

experimental variogram model because it requires quite a lot of data (Santos T.C and Yamamoto J.K., 2019). In the case of insufficient data available to construct an experimental variogram, there are other alternative methods that can be used to replace the geostatistical method, generally using a deterministic method (Yamamoto, 2002). Some important points in this study is that GIS is used for mapping because it can integrate and comparisons various data and information that resulting new insight

The objective of this research was to evaluate the performance of interpolation methods, deterministic global polynomial interpolation (GPI), Local polynomial interpolation (LPI), inverse distance weighted interpolation (IDW), and radial basis function (RBF), to determine the best deterministic method in mapping the spatial distribution of grades of Ni, Fe and Mg in the study area (Astari, A. J., et al, 2021).

2. RESEARCH METHOD

The research was undertaken on nickel laterite deposits of the limonite layer in the North Morowali district, Central Sulawesi Province (Figure 1.a). Geologically the research area is located in the ophiolite belt of Eastern Sulawesi (Fu et al, 2018). This ophiolite belt is part of the Circum Pacific phanerozoic ophiolite complex which was formed during the Cretaceous to Miocene (Hall and Wilson, 2000). The ophiolite belt consists of ultramafic rocks, mainly harzburgite, lherzolite, and peridotite (Fu et al, 2018, Simandjuntak et al, 1997). In the research area, most of the ultramafic rocks have been regionally metamorphosed to a moderate to high degree and the rocks are petrographically described as serpentinite (Fu et al, 2014). Intensive weathering of these ultramafic rocks can form one or more layers containing of nickel (Ni), iron (Fe), magnesium (Mg), cobalt (Co), and rarely scandium (Sc) (Butt and Cluzel, 2013, Brand et al, 1998).

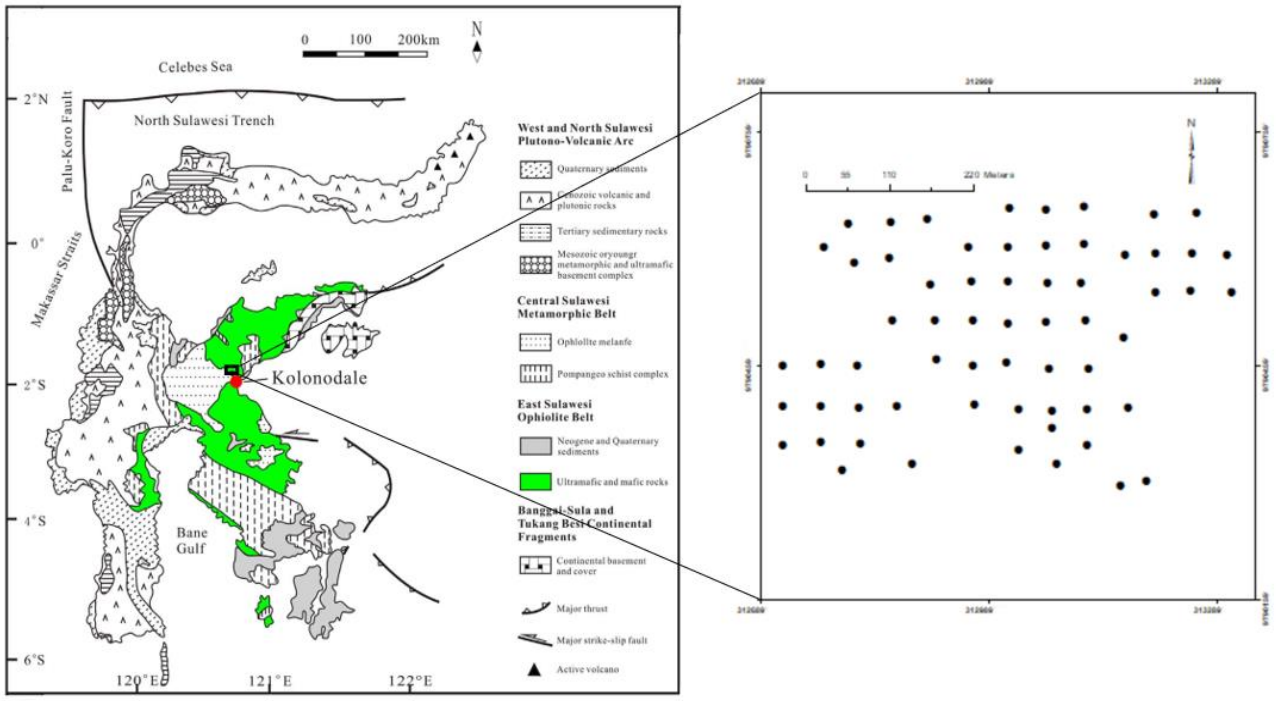

(a) (b)

Figure 1 (a) Regional Geology of Sulawesi (Fu et al, 2018), and (b) Location of the research area

This study uses data from exploration drilling in an area of ± (650 X 400) m². Drilling is carried out in a grid pattern with an average distance between drill points of 50m. A total of 62 drill holes (Figure.1.b) with limonite layer thickness ranging from 1m to 14m. Sampling for geochemical analysis was carried out at each drill hole at 1m intervals. Coordinates of the drill point locations

DOI: https://doi.org/10.17509/gea.v24i1.61886
p- ISSN 2776-608X e- ISSN 2776-5970

were determined using a global positioning system (GPS), while the analysis of Ni, Fe, and MgO were carried out using the XRF method.

Figure 2 is flowchart of data processing using the interpolation techniques that were applied to estimate the spatial distribution of Ni, Fe, and MgO grades, and evaluate the performance of each interpolation technique. It begins with visually analyzing the data by screening data values to identify inaccurate coordinates of sample locations, and illogical values of Ni, Fe and MgO analyzing results. The data used in processing is the composite value obtained from the results of calculating the weighted average value of each sample in each drill hole. Description of the data values and their distribution is presented in a summary of basic statistics, including minimum, maximum, average, standard deviation, coefficient of variance (CV), skewness, and amount of data. This composite database is then used to estimate locations where there is no measurement data, using inverse distance weighting (IDW), radial basis function (RBF), global polynomial interpolation (GPI), and local polynomial interpolation (LPI) interpolation techniques. The performance of each interpolation technique is then evaluated using the statistical parameters mean error (ME), root mean square error (RMSE), and mean relative error (MRE). The interpolation technique with the closest ME value to zero, and the lowest RMSE, or the lowest MRE value is the most optimum method (Jiang et al, 2022., Adhikary. P. P, and Dash. Ch. J., 2017).

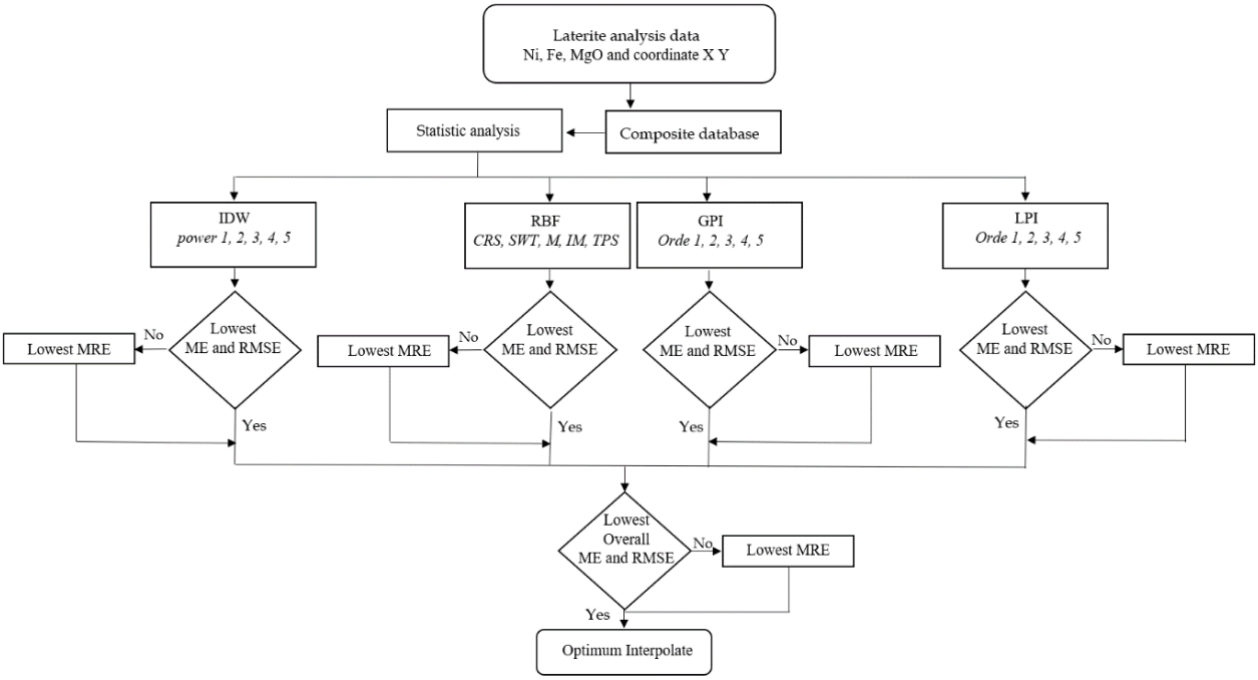

Figure 2. Model for prediction of Ni, Fe and MgO. IDW, inverse distance weighting; RBF, radial basis function; CRS, completely regularized spline; SWT, spline with tension; M, multiquadric; IM, inverse multiquadric; TPS, thin plate spline; GPI, global polynomial interpolation; LPI, local polynomial interpolation; ME, mean error; RMSE, root mean square error; MRE, mean relative error.

Spatial Interpolation Methods

There are two types of interpolation methods, namely global and local methods. In its interpolation the global method uses all data, observations in an area, are used for the estimation process and show trends in general, while the local method only uses data that is located around the estimated point (Li. J and Heap. A.D, 2008). In this research used global and local interpolation method, to generate spatial distribution maps of Ni, Fe, and MgO using a variety of deterministic interpolation techniques including; inverse distance weighting (IDW), radial basis function (RBF), global polynomial interpolation (GPI), and local polynomial interpolation (LPI).

DOI: https://doi.org/10.17509/gea.v24i1.61886
p- ISSN 2776-608X e- ISSN 2776-5970

a). Inverse Distance Weighting (IDW)

IDW is classified as local interpolator, and exact method which generate the same prediction as the observed value at the sample location point (Li and Heap, 2008). Even though other, more sophisticated interpolation methods have been developed, the IDW method is still widely used for spatial interpolation, because this method is simple, quick and easy to apply with satisfactory interpolation results (Cheng et al, 2017). This has been confirmed over the years in various research works from various disciplines (Gilewski, 2021). In its estimations, IDW gives values at an unsampled point based on the weighted average of the surrounding data values within the specified radius. The weight used in interpolation is a value that is inversely proportional to the distance between the unsampled point and the data location (Handoko. M, et.al, 2021). IDW will give less weight to data that is far from the unsampled location, and give greater weight to data that is located closer (Chen et al, 2017, Bhunia et al, 2016, Johnston et al, 2001). The IDW interpolation model is formulated as below:

$$w_i = \frac{\frac{1}{d_i^k}}{\sum_{i=1}^{n} \frac{1}{d_i^k}} w_i = \frac{\frac{1}{d_i^k}}{\sum_{i=1}^{n} \frac{1}{d_i^k}} \quad (1)$$

and,

$$\hat{Z}_0 = \sum_{i=1}^{n} w_i . Z_i \hat{Z}_0 = \sum_{i=1}^{n} w_i . Z_i \quad (2)$$

where $\hat{Z}_0 \hat{Z}_0$:estimated value at an unsampled location, $w_i w_i$: sample wight on site *I*, $d_i d_i$: distance between location *i* and unsampled location, kk:power parameters, $Z_i Z_i$: sample value on site *i.*

b). Radial Basis Function (RBF)

RBF is a series of exact, local interpolation techniques consisting of thin plate spline (TPS), spline with tension (SWT), multiquadric function (M), inverse multiquadric function (IM) and completely regularized spline (CRS). It can be imagined that the RBF is like a rubber sheet that is placed and fitted over the measured data points, by minimizing the total curvature of the rubber sheet passing through each data point (Bhunia et al, 2016). RBF interpolation is not effective if there is a dramatic change in data values over a short distance (Cheng and Xie, 2009). This method uses basic equations that depend on the distance between the estimated points and the location of the data points (Aguilar et al, 2005). If Z is the predicted value, then RBF is can be formulated as below (Adhikary. P. P, and Dash. Ch. J., 2017):

$$Z = \sum n\ i=1 \lambda i \phi(|x - xi\ |) + p(x) \quad (3)$$

where p(x): function of the polynomial, λi: weight, |x-xi|: represent the Euclidean distance between x and the center point xi, and φ: radial basis function

c). Global Polynomial Interpolation (GPI)

GPI is a deterministic method, inexact, and global interpolation, which in its predictions uses mathematical functions, first, second, third degree, or higher degree (Cooper et al, 2015). This method is suitable for applying data values with gradual variations, but is prone to outliers, especially at the edges of the study area (Johnston et al, 2001). In its prediction, GPI uses the entire data population in the area of interest, and its interpolation produces gradual surface variations (Wang, 2014). In applying this method, it is necessary to pay attention to the degree of the polynomial used to adjust the surface of the data values (Antal et al, 2021). The first order GPI interpolation technique is calculated based on the following equation (Tanjung et al, 2020):

DOI: https://doi.org/10.17509/gea.v24i1.61886
p- ISSN 2776-608X e- ISSN 2776-5970

$$Zxy = b0 + b1x + b2y \qquad (4)$$

In this study, testing was carried out using the level of order polynomial values 1 to order 5.

d). Local Polynomial Interpolation (LPI)

LPI is a moderately quick deterministic method, inexact and local interpolation. When compared to GPI, this method is a more flexible interpolator (Johnston et al, 2001). In its prediction, it is not like GPI which uses all population data, but uses data around the predicted location which is specifically determined by the operator (Wang et al, 2014). In its estimation, LPI uses several parameters including the maximum and minimum amount of surrounding data, environment type, sector, and kernel type, such as for example; exponential, gaussian, quartic and constant (Johnston et al, 2001). LPI prediction results are more accurate when used in smaller areas, locations between data have the same distance and are normally distributed (Luo et al, 2008). In its calculations, LPI uses polynomial equations for all types of kernels. The weight of the prediction (W_i) can be calculated by the following equation (Antal et al, 2021):

$$W_i = \left(1 - \frac{d_i}{R}\right) p \qquad (5)$$

Where d_i is the distance between the data and the predicted location, R represents the area where the data is taken in the estimation, and p is a sequence of polynomial functions determined by the operator.

e). Performance Comparison of The Interpolation Method

To evaluate the performance of the IDW, RBF, GPI, and LPI interpolation methods, cross validation techniques are used. This method has been widely used in various fields of science (Jiang et al, 2022), including in the fields of earth sciences and mining sector. This technique is also known as "leave-one-out cross validation", and this method is part of the Monte Carlo group (Berrar, 2018). The CV procedure is carried out in two stages: First, temporarily removing one of the observation data from the data set, then at the point where the observation value has been deleted it is predicted using other observational data. Second, the predicted value at that point is compared with the actual observed value. This procedure is carried out repeatedly and sequentially on all observational data in the data set (Antal et al, 2021). The results of the comparison allow for discrepancies between predicted data ($\hat{Z}(x_i)$) and observed data ($Z(x_i)$), which is expressed in experimental error (E).

$$E = \hat{Z}(x_i) - Z(x_i) \qquad (6)$$

Evaluation of the prediction results from the interpolation method can be determined by the value of the difference between the observed data and the value of the interpolation results (Antal et al, 2021). In this study, to test the performance of each interpolation method, the indicators mean error (ME), root mean square error (RMSE), and mean relative error (MRE) are used. The ME indicator shows the average difference between the predicted value and the observed value. The ME value indicates the bias of the prediction, if the interpolation is accurate or unbiased, the ME value is equal to zero (Johnston et al, 2001). The ME equation model is expressed as follows:

$$ME = \frac{1}{n}\sum_{i=1}^{n}[Z(x_i) - \hat{Z}(x_i)] ME = \frac{1}{n}\sum_{i=1}^{n}[Z(x_i) - \hat{Z}(x_i)] \qquad (7)$$

Meanwhile, the RMSE value indicates the accuracy of the prediction results, where the predicted results are stated to be more accurate if they have a smaller RMSE value. The RMSE value is calculated according to the following equation (Arkoc, 2021., Cheng et al, 2017):

DOI: https://doi.org/10.17509/gea.v24i1.61886
p- ISSN 2776-608X e- ISSN 2776-5970

$$RMSE = \left[\frac{1}{n}\sum_{i=1}^{n} \left(\hat{Z}_{(x_i)} - Z_{(x_i)}\right)^2\right]^{0.5} \qquad (8)$$

The MRE indicator is used if the ME and RMSE values show a discrepancy, where the prediction results are stated to be more accurate if the MRE value is smaller (Adhikary. P. P, and Dash. Ch. J., 2017). The MRE model is expressed as follows:

$$MRE = \frac{RMSE}{\delta} \qquad (9)$$

where $\hat{Z}(x_i)\hat{Z}(x_i)$: estimated value, $Z(x_i)Z(x_i)$: measurement value, nn n: amoun of predictive data, and δ is the difference between the maximum and minimum values of the observation data.

3. RESULTS AND DISCUSSION

a) Descriptive Statistical Analysis

The data base used in this research is composite data of Ni, Fe, and MgO from each drill hole in the limonite layer. A description of the statistical analysis of the composite data is presented in Table 1. The statistical analysis showed that the standard deviation values were lower for Ni (0.21) and higher for MgO (4.15) and Fe (9.29). In addition, coefficient of variance (CV) shows a low value for Ni (0.19) and Fe (0.28) that indicate low data variability (Yasrebi et al, 2009), but showed high variability for MgO (0.71). Likewise, the coefficient of skewness shows varying values of Fe (-0.5), Ni (0.66), and MgO (1.08). To fit the data into a normal distribution, a logarithmic transformation needs to be considered for MgO with a coefficient of skewness > 1 (Webster and Oliver, 2001), and CV > 0.5 (Annels A.E., 1991).

Table 1: Description of the statistical analysis of Ni, Fe and MgO grades

Element	Min	Max	Mean	Std dev	CV	Skew	N
Ni	0.7	1.85	1.12	0.21	0.19	0.66	62
Fe	11.22	33.01	33.01	9.29	0.28	-0.50	62
MgO	0.30	19.01	5.81	4.15	0.71	1.08	62

Min: Minimum value, Max: Maximum value, Std dev: Standard deviation, CV: Coefficient of variation, Skew: *Skewness*, N: Amount of composite data.

b) Spatial Interpolation

Estimation of Ni, Fe and MgO with the IDW method uses composite data with equations (1) and (2). In the calculations, the power value is manipulated from one to five and the data included in the calculation is a minimum of 3 and a maximum of 15. For the prediction using the RBF method, consisting of CRS, SWT, M, IM, and TPS, using equation (3) with the number of data used a minimum of 3 and a maximum of 15. While the estimation using the GPI and LPI methods uses the order of 1 to 5. Calculating the GPI uses the entire data population, as many as 62 data, with using equation (4). In the LPI method, the amount of data used in the calculation is a maximum of 15 and a minimum of 3 data with using equation (6).

c) Performance Analysis

Performance analysis of the interpolation methods for Ni

The performance results of the methods used in interpolating Ni grades were obtained from the cross-validation process, the comparison of the errors of the interpolation is presented in table 2.

DOI: https://doi.org/10.17509/gea.v24i1.61886
p- ISSN 2776-608X e- ISSN 2776-5970

The mean error (ME) values close to 0 indicate a small bias (Arkoc, 2021., Cheng et al, 2017), and smaller values of root mean square error (RMSE) and mean relative error (MRE) indicates a more accurate prediction (Adhikary. P. P, and Dash. Ch. J., 2017). The cross-validation results in table 2 show that the interpolation results of the IDW method with the lowest RMSE and MRE values were obtained in the IDW power 1 technique (RMSE=0.2286479, MRE=0.1983930). This shows that the prediction results of the IDW power 1 method are more accurate than those of IDW power 2, power 3, power 4, and IDW power 5. For the RBF method the best interpolation result is the IM technique with a value of RMSE=0.2181237, and MRE=0.1892613 as the lowest value when compared with the CRS, SWT, M, and TPS techniques. For the GPI and LPI methods, the results of interpolation with the lowest RMSE and MRE values occurred at 1st order GPI with RMSE=0.2263752 and MRE=0.1964210, and 1st order LPI with RMSE=0.2292902, and MRE=0.1989503.

From the four interpolation methods, it is found that the order of the RMSE values is as follows: RBF (IM) < GPI (Order 1) < IDW power1 < LPI (order 1). Likewise, the MRE values show the same sequence of values, namely: RBF (IM) < GPI (order 1) < IDW power1 < LPI (order 1). This shows that the prediction results for the value of Ni using the RBF (IM) interpolation method are better than the GPI, IDW, and LPI methods.

Table 2: Comparison of the errors of the interpolation methods to estimate Ni grade

Interpolation Method		Element	ME	RMSE	MRE
IDW	Power-1	Ni	-0.0070855	0.2286479	0.1983930
	Power-2		-0.0029475	0.2421897	0.2101429
	Power-3		0.0003916	0.2545743	0.2208888
	Power-4		0.0023933	0.2632794	0.2284420
	Power-5		0.0034524	0.2686419	0.2330949
RBF	Compl Regularized S	Ni	-0.0043061	0.2493090	0.2163202
	Spline with Tension		-0.0048804	0.2439072	0.2116332
	Multiquadric		-0.0033472	0.2978907	0.2584735
	Inverse Multiquadric		-0.0108120	0.2181237	0.1892613
	Thin Plate Spline		-0.0060555	0.3583383	0.3109226
GPI	Orde 1	Ni	-0.0011512	0.2263752	0.1964210
	Orde 2		-0.0011224	0.2361267	0.2048822
	Orde 3		-0.0043199	0.2619525	0.2272907
	Orde 4		-0.0085367	0.3175354	0.2755181
	Orde 5		-0.0186640	0.3517350	0.3051931
LPI	Orde 1	Ni	0.0065858	0.2292902	0.1989503
	Orde 2		-0.0022503	0.2481513	0.2153156
	Orde 3		-0.0073209	0.2855512	0.2477668
	Orde 4		-0.0132080	0.3301447	0.2864596
	Orde 5		-0.0174260	0.3884991	0.3370925

Visualization of the spatial distribution of the best predicted results for Ni grades in each of the IDW, RBF, GPI, and LPI interpolation methods are presented in Figure 3. The four map images show different distribution patterns of Ni grade variations, where the IDW method interpolation results show the Ni grade distribution pattern is the most varied (Figure 3a), but in general the interpolation results from the four methods show that most of the study area is occupied by laterite deposits with

DOI: https://doi.org/10.17509/gea.v24i1.61886
p- ISSN 2776-608X e- ISSN 2776-5970

a content of 1-1.2% Ni (green color). In fact, the results of the interpolation of the GPI method show that the entire study area is occupied by a distribution of Ni grades in the range of 1-1.2%. The best interpolated map using the RBF method (Figure 3b) shows the distribution of laterite with a range of 1-1.2% Ni occupying an area of ± 95% and a range of 1.2-1.5% Ni occupying an area of ± 5% in the northeastern part of the study area.

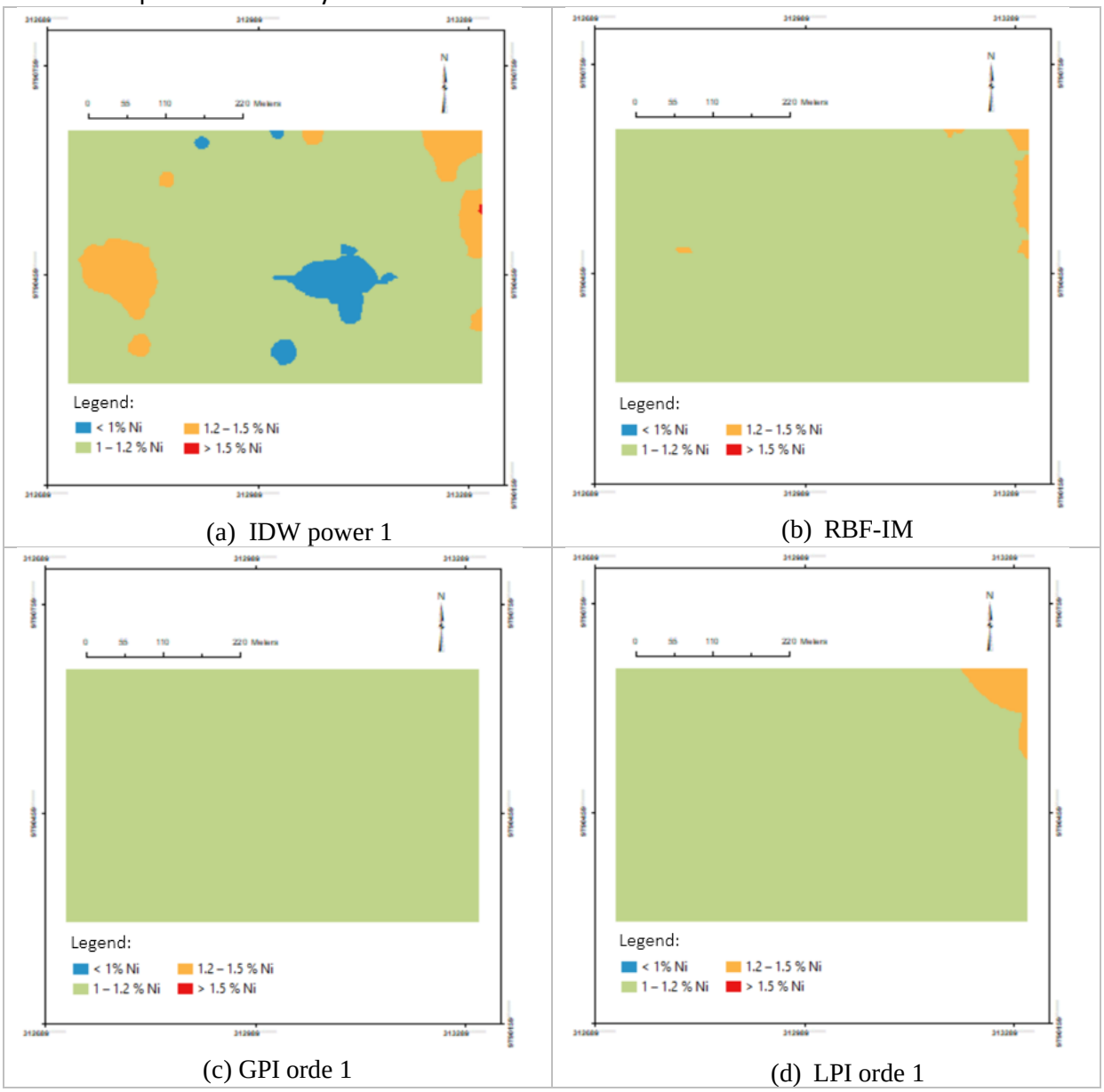

Figure 3: Map of the distribution of Ni grade with the best interpolation results from the IDW, RBF, GPI and LPI methods

Performance analysis of the interpolation methods for Fe

The results of the cross validation of Fe (Table 3) show that the interpolation of the IDW method with the lowest RMSE and MRE values occurs at IDW power 2 (RMSE=8.6364075, and MRE=0.2111642). This shows that the interpolation results of the IDW power 2 is more accurate than the IDW power 1, IDW power 3, IDW power 4, and IDW power 5. For the RBF method the best interpolation results are shown by the IM technique with the smallest RMSE and MRE values (RMSE=8.4544950, MRE=0.2067164) if compared to the CRS, SWT, M, and TPS techniques. For the GPI method the results of interpolation with the lowest RMSE and MRE values occur at order 3

DOI: https://doi.org/10.17509/gea.v24i1.61886
p- ISSN 2776-608X e- ISSN 2776-5970

(RMSE=9.1413733 and MRE=0.2235109), while for the LPI method the lowest RMSE and MRE values occur at LPI order 2 (RMSE=9.0299247, and MRE=0.2207859).

Comparison of the four interpolation methods shows that the RMSE and MRE values are as follows: RBF (IM) < IDW-power 2 < LPI-order 2 < GPI-order 3. These results indicate that the estimated value of Fe using the RBF interpolation method (IM) is better than the IDW, LPI, and GPI methods.

Table 3: Comparison of the errors of the interpolation methods to estimate Fe grade

Interpolation Method		Element	ME	RMSE	MRE
IDW	Power-1	Fe	0.0439905	8.5870638	0.2099577
	Power-2		0.2408631	8.6364075	0.2111642
	Power-3		0.3441666	8.7460275	0.2138445
	Power-4		0.4006154	8.8666945	0.2167948
	Power-5		0.4312016	8.9925964	0.2198732
RBF	Compl Regularized Spline	Fe	-0.0099677	8.4964732	0.2077428
	Spline with Tension		-0.0220568	8.5067450	0.2079939
	Multiquadric		0.1939755	8.8676131	0.2168173
	Inverse Multiquadric		-0.0648856	8.4544950	0.2067164
	Thin Plate Spline		0.0493249	9.8016668	0.2396554
GPI	Orde 1	Fe	-0.0155602	9.3799477	0.2293441
	Orde 2		0.0776022	9.5515352	0.2335395
	Orde 3		0.2089692	9.1413733	0.2235109
	Orde 4		0.0588232	9.3764661	0.2292590
	Orde 5		0.1561032	11.934502	0.2918042
LPI	Orde 1	Fe	0.3562450	9.0500386	0.221277
	Orde 2		-0.0323120	9.0299247	0.2207859
	Orde 3		0.1338178	9.0799835	0.2220099
	Orde 4		0.2804415	9.7993732	0.2395993
	Orde 5		0.3687216	11.069589	0.2706567

Visualization of the spatial distribution of Fe grade as the best predictor of the IDW, RBF, GPI, and LPI interpolation methods is presented in Figure 4. The results of the four interpolation methods show different distribution patterns, but in general laterite deposits with a grade range of 25–35% Fe (green color on the map) occupy a larger area than the distribution of grades with other ranges.

The best interpolated map using the RBF method (Figure 4b), shows that laterite distribution with a grade range of 11-25% Fe occupies an area of ±15% (blue color), a range of 25-35% Fe occupies an area of ±45% (green color), 35-42% Fe occupies an area of ±30% (orange color), and Fe > 42% occupies an area of ±10% of the study area (red color).

DOI: https://doi.org/10.17509/gea.v24i1.61886
p- ISSN 2776-608X e- ISSN 2776-5970

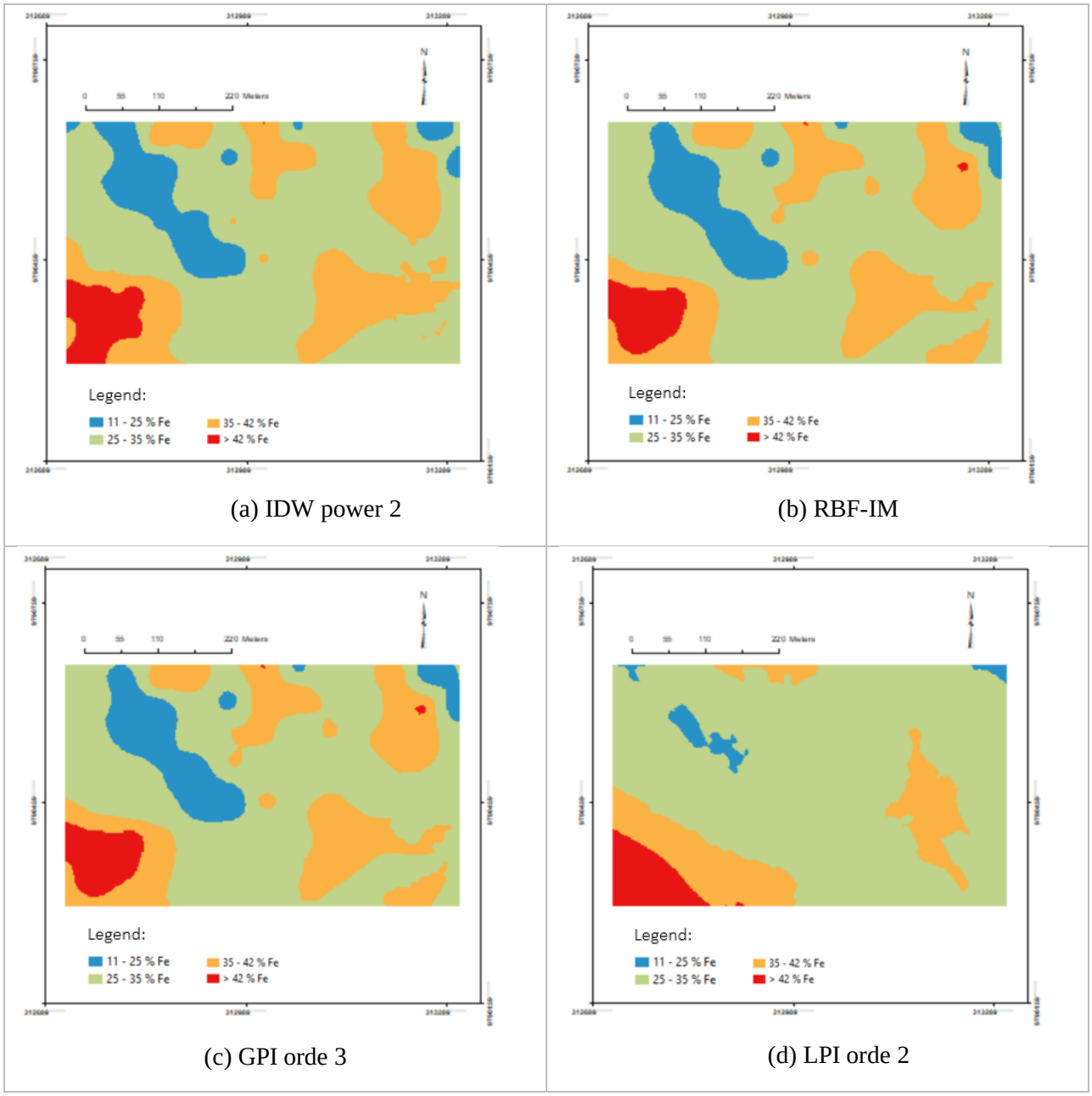

Figure 4. Map of the distribution of Fe grade with the best interpolation results from the IDW, RBF, GPI, and LPI methods.

Performance analysis of the interpolation methods for MgO

A comparison of the error values from the cross-validation results for MgO grades (Table 4) shows that the best IDW interpolation results are IDW power 1. This is indicated by the RMSE=3.727657181 and MRE=0.199233414 values which are the smallest when compared to the RMSE and MRE values at IDW power 2, power 3, power 4, and IDW power 5. Meanwhile, the best interpolation results for the RBF method were shown by the IM technique with values of RMSE=3.6994800 and MRE=0.1977274 which are the smallest values when compared to the CRS, SWT, M, and TPS techniques.

For the GPI method, the best interpolation results are the 3rd order GPI with a value of RMSE=3.8905849 and MRE=0.2079414, while the best LPI method is the 1st order LPI technique with a value of RMSE=3.8661828 and MRE=0.2066372.

A comparison of the four interpolation methods applied in the study area showed that the estimated distribution of MgO grades using the RBF (IM) method was better than the IDW, LPI, and

DOI: https://doi.org/10.17509/gea.v24i1.61886
p- ISSN 2776-608X e- ISSN 2776-5970

GPI methods. This is shown by the smallest RMSE and MRE values in the RBF method when compared to the IDW-power 1, LPI-order 1, and GPI-order 2 techniques.

Table 4. Comparison of the errors of the interpolation methods to estimate MgO grade

Interpolation Method		Element	ME	RMSE	MRE
IDW	Power-1	MgO	0.0096039	3.7276571	0.1992334
	Power-2		-0.0451281	3.8100258	0.2036358
	Power-3		-0.0725341	3.9003281	0.2084622
	Power-4		-0.0886117	3.9764416	0.2125302
	Power-5		-0.0993768	4.0451118	0.2162005
RBF	Compl Regularized Spline	MgO	0.0214197	3.7552893	0.2007102
	Spline with Tension		0.0313820	3.7389791	0.1998385
	Multiquadric		-0.0292977	3.9962945	0.2135913
	Inverse Multiquadric		0.0929783	3.6994800	0.1977274
	Thin Plate Spline		0.0550910	4.5312660	0.2421841
GPI	Orde 1	MgO	0.0055294	3.9336026	0.2102406
	Orde 2		-0.0280796	4.0896807	0.2185826
	Orde 3		-0.0623202	3.8905849	0.2079414
	Orde 4		0.0006526	4.0286447	0.2153204
	Orde 5		-0.0203266	5.2112062	0.2785251
LPI	Orde 1	MgO	-0.1213830	3.8661828	0.2066372
	Orde 2		0.0397288	3.8820701	0.2074863
	Orde 3		-0.0427943	3.9513313	0.2111882
	Orde 4		0.0109751	4.3553737	0.2327832
	Orde 5		-0.0203905	5.4361406	0.2905473

Spatial distribution map of MgO best predicted results from the IDW, RBF, GPI, and LPI interpolation methods is presented in Figure 5. In general, the distribution pattern of MgO grades predicted from the four interpolation methods shows almost the same pattern, where the distribution of high MgO grades is in the range of 6.5 –19 % (red color) occupies the northeastern and northwestern parts of the study area. The best interpolated map, using the RBF method (Figure 5b), shows that the distribution of MgO grades in the range of 6.5-19% occupies an area of ±45% (red color) in the northwestern and northeastern parts of the research area. For the MgO in the range of 4.5-6.5% occupy an area of ±35% (orange color) in the north and narrow in the south, while MgO levels with a range of 2.5-4.5% occupy an area of ±15% (green color) in the south, and low levels of MgO in the range of 0.3-2.5% occupy an area of ±5% in the southwestern part of the study area (blue color).

DOI: https://doi.org/10.17509/gea.v24i1.61886
p- ISSN 2776-608X e- ISSN 2776-5970

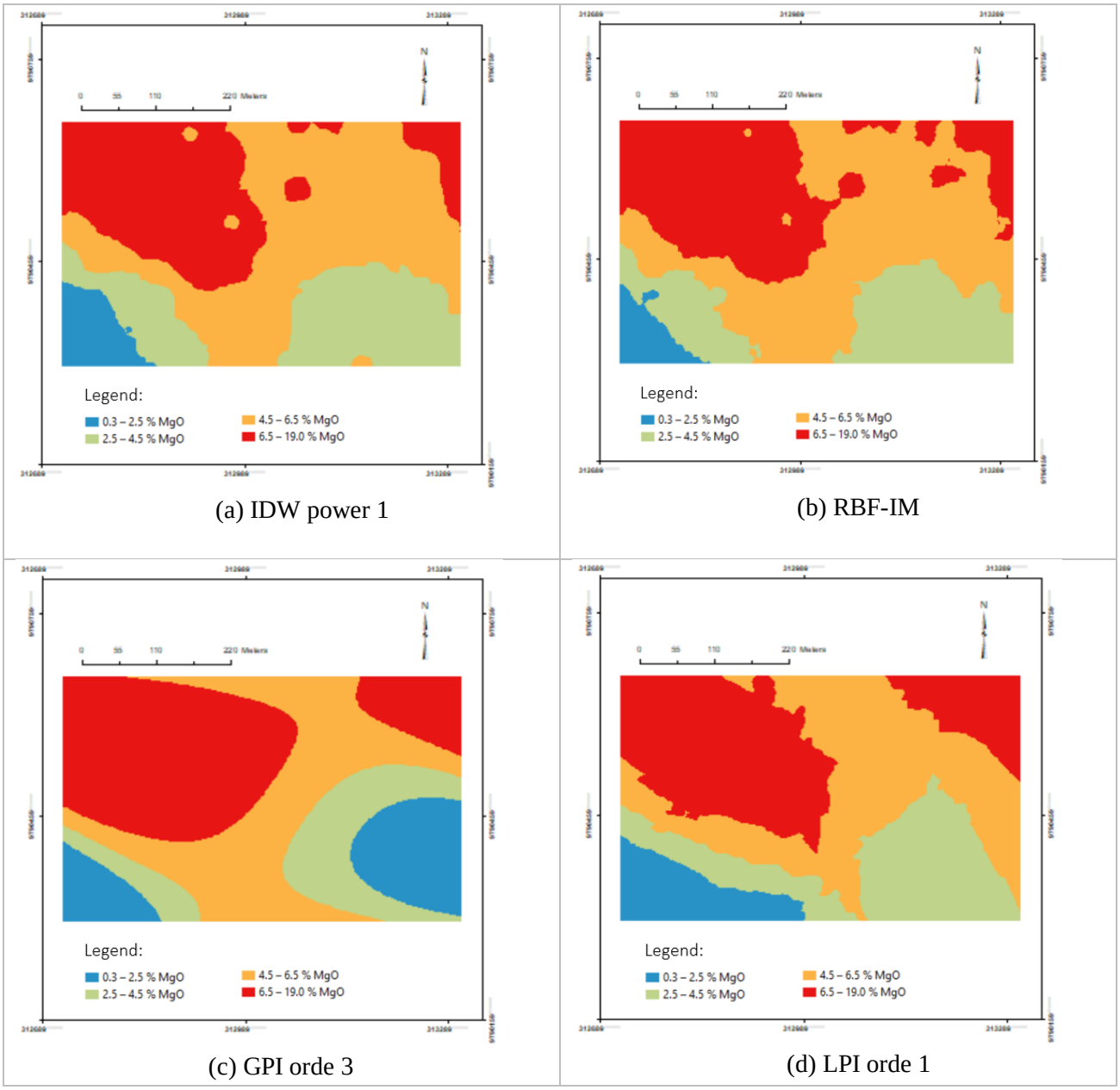

Figure 5. Map of the distribution of MgO grade with the best interpolation results from the IDW, RBF, GPI and LPI methods

4. CONCLUSIONS

Comparison of local deterministic (IDW, RBF, LPI), and global deterministic (GPI) interpolation methods to predict Ni, Fe and MgO grades in the research area was carried out using ME, RMSE, and MRE statistical parameters. In the research area, the RBF method showed the best performance for predicting the distribution of Ni, Fe and MgO grades compared to other deterministic interpolation methods. Cross validation measurements of Ni grades show that the performance of the RBF interpolation method is sequentially better than GPI, IDW, and LPI. For Fe and MgO grades the performance of the RBF interpolation method was better than IDW, LPI and GPI.

5. REFERENCES

Adhikary. P. P, and Dash. Ch. J., 2017, Comparison of deterministic and stochastic methods to predict spatial variation of ground water depth, *Appl Water Sci, 7*: 339-348.

DOI: https://doi.org/10.17509/gea.v24i1.61886
p- ISSN 2776-608X e- ISSN 2776-5970

Aguilar. F.J, Aguera. F, Aguilar. M.A, Carvaja. F., 2005, Effect of terrain morphology, sampling density, and interpolation methods on Grid DEM accuracy, *Photogrametric Engineering & Remote Sensing 71* (7), 805-816.

Annels. A. E., 1991, Mineral Deposit Evaluation, A practical approach, *Chapman & Hall*.

Antal. A, Guerreiro. P.M.P, Cheval. S., 2021, Comparison of spatial interpolation methods for estimating the precipitation distribution in Portugal, *Theoretical Applied Climatology, 145*: 1193-1206.

Arkoc. O., 2021, Modeling of spatiotemporal variations of groundwater levels using different interpolation methods with the aid of GIS, case study from Ergene Basin, Turkey, *Modeling Earth System and Environment.*

Astari, A. J., Mohamed, A. A. A., & Ridwana, R. (2021). The Role of Geographic Information Science in Achieving Sustainable Development Goals (SDGs) During the Covid-19 Pandemic. *Jurnal Geografi Gea, 21*(2), 112-122.

Berrar. D., 2018., Cross-validation, *Reference Module in Life Sciences*.

Bhunia. G.S, Shit. P.K, Maiti. R., 2016, Comparison of GIS-based interpolation methods for spatial distribution of soil organic carbon (SOC), *J Saudi Soc Agric Sci*.

Brand. N.W, Butt. C.R.M, Elias M., 1998, Nickel lateritic: classification and features. AGSO J. Aust. Geol. *Geophys, 17*(4), 81-88.

Butt. C. R. M, and Cluzel. D., 2013, Nickel Laterite Ore Deposits: Weathered Serpentinites, *Elements, Vol.9*, pp. 123-128.

Chai. H, Cheng W, Zhou C, Chen X, Ma X, Zou S., 2011, Analysis and comparison of spatial interpolation methods for temperature data in Xinjiang Uygur Autonomous Region, China, *Nat Sci 3*(12): 999-1010.

Chen. T, Ren. L, Yuan. F, Yang. X, Jiang. S, Tang. T, Liu. Y, Zhao. C, and Zhang. L.,2017, Comparison of spatial interpolation schemes for rainfall data and application in hydrological modeling, *Water, 9*, 342.

Cheng. M, Wang. Y, Engel. B, Zhang. W, Peng. H, Chen. X, Xia. H., 2017, Performance assessment of spatial interpolation of precipitation for hydrological process simulation in the Three Georges Basin, *Water 9*, 838.

Cheng. X.F, and Xie. Y., 2009 Spatial distribution of soil organic carbon density in Anhui Province based on GIS, *Sientia Geograph. Sin 29* (4) 540-544.

Cooper. H.M, Zhang. C, Selch. D., 2015, Incorporating uncertainty of groundwater modeling in se-level rise assessment, A case study in South Florida, *Climatic Change, 129* (1-2), pp 281-294.

Daya. A. A., 2012, Reserve estimation of central part of Choghart north anomaly iron ore deposit through ordinary kriging method, *International Journal of Mining and Technology 22*, 573-577.

Elias M., 2002, Nickel laterite deposits-Geological overview, resources and exploration, *Cent. Ore depos. Res. Univ Tasmania* 205-220.

Fu. W, Zhang. Y, Pang. C, Zeng. X, Huang. X, Yang. M, Shao. Y, Lin. H., 2018, Garnierite mineralization from a serpentinite-derived lateritic regolith, Sulawesi Island, Indonesia;

DOI: https://doi.org/10.17509/gea.v24i1.61886
p- ISSN 2776-608X e- ISSN 2776-5970

mineralogy, geochemistry ang link to hydrologic flow regime, *Journal of Geochemical exploration 188*, p. 240-256.

Fu. W, Yang. J. W, Yang. M. L, Pang. B. C, Liu. X. J, Niu. H. J, Huang. X. R., 2014, Mineralogical and geochemical characteristics of a serpentinite-derived lateritic profile from East Sulawesi, Indonesia: implications for the laterization process and Ni supergene enrichment in the tropical rainforest. *Journal Asian Earth Sci. 93*, p74-88.

Farrokhpay S, Cathelineau M, Blancher S B, Laugier O, Filippov L., 2019, Characterization of Weda Bay nickel laterite ore from Indonesia, *J Geochem Explor 196*: 270-281.

Garvin. M M, Simon. M.J., 2014, A detail assessment of global nickel resource trends and endowments, *Soc. Econ, Geol. Inc. Ecom. Geol, 109*, 1813-1814.

Gilewski. P., 2021, Impact of the grid resolution and deterministic interpolation of precipitation on rainfall-runoff modeling in a sparsely gauged mountainous catchment, *Water, 13*, 230, p. 1-21.

Golightly J., 1981, Nickeliferous laterite deposits, *Econ. Geol, 75*, 710-735.

Guo. Z, Zhu. D, Pan. J, Zhang. F., 2017, Mineralogical characteristics and preliminary beneficiation of nickel slag from reduction roasting-ammonia leaching, *Minerals 7*:98-114.

Hall. R, E. J. Wilson., 2000, Neogene Suture in Eastern Indonesia, *Journal Asian Earth Sci, 18*, p. 781-808.

Handoko, M., & Sutrisno, A. J. (2021). Spatial and Temporal Analysis of Dissolved Oxygen (DO) and Biological Oxygen Demand (BOD) Concentration in Rawa Pening Lake, Semarang Regency. *Jurnal Geografi Gea, 21*(1), 58-71.

Isdianti, A. R., Ibrahim, E., & Setiawan, B. (2022). Soil erodibility in post coal mining land reclamation area in backfilling MTBU Tambang Air Laya (TAL) PT Bukit Asam Tbk., Tanjung Enim Mining Unit (UPTE) Muara Enim, South Sumatera. *Jurnal Geografi Gea, 22*(1), 47-54.

Jiang. B, Xu. W, Zhang. D, Nie. F, Sun. Q., 2022, Contrasting multiple deterministic interpolation responses to different spatial scale in prediction soil organic carbon: A case study in Mollisols regions, *Ecological Indicators 134* (2022) 108472, p 1-11.

Johston. K, VerHoef. J. M, Krivoruchko. K, Lucas. N., 2001, Using ArcGIS geostatistical analyst, Redlands, CA, USA: *ArcGIS Manual by ESRI*.

Konig. U., 2021, Nickel laterites-mineralogical monitoring for grade definition and process optimization, *minerals, 11*, 1178.

Li. J, and Heap. A.D.,2008, A review of spatial interpolation methods for environmental scientists, Canberra. *Geocience Australia Record 208*/23, 137 pp.

Li X L, Xie Y L, Guo Q J, Li L H., 2010, Adaptive ore grade estimation method for the mineral deposit evaluation, *Mathematical and Computer Modelling 52*. 1947-1956.

Losser T, Li L, Piltner R A., 2014, Spatio temporal interpolation method using radial basis functions for geospatio temporal big data, In IEEE fifth international conference on computing for geospatial research and application, *COM. GEO* pp 17-24.

DOI: https://doi.org/10.17509/gea.v24i1.61886
p- ISSN 2776-608X e- ISSN 2776-5970

Luo. W, Taylor. M.C, Parker. S.R., 2008, A comparison of spatial interpolation methods to estimate continuous wind speed surface using irregular distributed data from England and Wales, *Int Journal Climatology 28* (7): 947-959.

Nkrumah P N, Baker A J. M, Chaney R L, Erskine P D, Echevarria G, Morel J l, Ent A V D., 2016, Current status and challenges in developing nickel Phyto mining: an agronomic perspective*, Plant Soil 406*: 55-69.

Qu H, Liu H, Tan K, Zhang Q., 2021, Geological feature modeling and reserve estimation of uranium deposits based on multiple interpolation methods, *Processes, 10*, 67, pp 1-16.

Santos T.C and Yamamoto J.K., 2019, Ore resource estimation based on radial based functions - Case study on Uniao Luiz and Morro do Carrapato gold deposits (Alta Floresta gold province), REM, int. Eng. J., Ouro Preto, 72(3), 493-499.

Simandjuntak T.O, Surono, Supardjono J.B., 1997, Geology map of the Poso quadrangle, Sulawesi, *Geological Research and Development Centre*, Bandung, Scale 1: 250,000.

Tanjung. M, Syahreza. S, Rusidi. M., 2020, Comparison of interpolation methods based on Geografic Information system (GIS) in the spatial distribution of seawater intrusion, *Jurnal Natural vol.20*, (2).

Wang. S, Huang. G.H, Lin. Q.G, Li. Z, Zhang. H, and Fan. Y.R, 2014, Comparison of interpolation methods for estimating spatial distribution of precipitation in Ontario, Canada, *Int. J, Climatol. 34*: 3745-3751.

Webster R, and Oliver M.A., 2001, Geostatistics for environmental scientists, *John Wiley and Sons*, Brisbane, Australia.

Yamamoto J.K., 2002, Ore reserve estimation using radial basis function, *Rev. do Instituto Geologico, v.23*, n.1, p.25-38.

Yan N, Zhao X L, Zhao S G, Zheng H W., 2015, Research progress on sample preparation methods and analytical techniques for nickel laterite, *Rock Miner Anal 34*: 1-11.

Yasrebi. J, Saffari. M, Fathi. H, Karimian. N, Moazallahi. M, Gazni. R., 2009, Evaluation and comparison of ordinary kriging and inverse distance weighting methods for prediction of spatial variability of some soil chemical parameters, *Research Journal of Biological Sciences 4* (1): 93-102.

Yong X, Xiaomin G, Shiyang Y, Jingli S, Yali C, Qiulan Z, Yong N., 2016, Geostatistical interpolation model selection based on ArcGIS and spatio-temporal variability analysis of ground water level in piedmont plains, northeast China, *Springer Plus* pp 1-15.

Zhang J.D, Wang C, Yu S.Q, Chen S.D, Guo S.M, Ding M.S, Tan H.Z., 2002, Exploration specifications on in-situ leaching sandstone type uranium deposits; standard No. EJ/T1157-2002, *National defense science, Technology and Industry commission*, Beijing, China.

Zhang Y, Qie J, Wang X F, Cui K, Fu T, Wang J, Qi Y., 2019, Mineralogical characteristics of the nickel laterite, southeast ophiolite belt, Sulawesi Island, Indonesia, Mining, Metallurgy & exploration.

Zhou S W, Wei Y G, Li B, Wang H, Ma B Z, Wang C Y, Lou X., 2017, Mineralogical Characterization and design of a treatment process for Yunan nickel laterite ore, China *Int J Miner Process 159*: 51-59.

DOI: https://doi.org/10.17509/gea.v24i1.61886
p- ISSN 2776-608X e- ISSN 2776-5970